Environmental Pollution 248 (2019) 496–505

Contents lists available at ScienceDirect

Environmental Pollution

journal homepage: www.elsevier.com/locate/envpol

Impacts of peat-forest smoke on urban $PM_{2.5}$ in the Maritime Continent during 2012–2015: Carbonaceous profiles and indicators☆

Jackson Tham [a, b], Sayantan Sarkar [a, 1], Shiguo Jia [a, b, 2], Jeffrey S. Reid [c], Shailendra Mishra [a, d], I.M. Sudiana [e], Sanjay Swarup [a, d], Choon Nam Ong [a], Liya E. Yu [a, b, *]

[a] NUS Environmental Research Institute, National University of Singapore, 5A Engineering Drive 1, 117411, Singapore
[b] Department of Civil and Environmental Engineering, National University of Singapore, 1 Engineering Drive 2, 117576, Singapore
[c] Naval Research Laboratory, Monterey, CA, 93943-5502, USA
[d] Department of Biological Sciences, National University of Singapore, 14 Science Drive 4, 117543, Singapore
[e] Cibinong Science Center, LIPI, Jl. Raya Bogor Km 46, Cibinong Bogor, 16911, Indonesia

ARTICLE INFO

Article history:
Received 21 November 2018
Received in revised form
15 February 2019
Accepted 15 February 2019
Available online 20 February 2019

Keywords:
Biomass burning
Peat forest smoke indicator
OCEC fraction
Southeast Asia
Organic aerosol

ABSTRACT

This study characterizes impacts of peat-forest (PF) smoke on an urban environment through carbonaceous profiles of >260 daily $PM_{2.5}$ samples collected during 2012, 2013 and 2015. Organic carbon (OC) and elemental carbon (EC) comprising eight carbonaceous fractions are examined for four sample groups – non-smoke-dominant (NSD), smoke-dominant (SD), episodic $PM_{2.5}$ samples at the urban receptor, and near-source samples collected close to PF burning sites. PF smoke introduced much larger amounts of OC than EC, with OC accounting for up to 94% of total carbon (TC), or increasing by up to 20 times in receptor $PM_{2.5}$. SD $PM_{2.5}$ at the receptor site and near-source samples have OC3 and EC1 as the dominant fractions. Both sample classes also exhibit char-EC >1.4 times of soot-EC, characterizing smoldering-dominant PF smoke, unlike episodic $PM_{2.5}$ at the receptor site featuring large amounts of pyrolyzed organic carbon (POC) and soot-EC. Relative to the mean NSD $PM_{2.5}$ at the receptor, increasing strength of transboundary PF smoke enriches OC3 and OC4 fractions, on average, by factors of >3 for SD samples, and >14 for episodic samples. A peat-forest smoke (PFS) indicator, representing the concentration ratio of (OC2+OC3+POC) to soot-EC, shows a temporal trend satisfactorily correlating with an organic marker (levoglucosan) of biomass burning. The PFS indicator systematically differentiates influences of PF smoke from source to urban receptor sites, with a progressive mean of 3.6, 13.4 and 20.1 for NSD, SD and episodic samples respectively at the receptor site, and 54.7 for the near-source $PM_{2.5}$. A PFS indicator of $\geq$5.0 is proposed to determine dominant influence of transboundary PF smoke on receptor urban $PM_{2.5}$ in the equatorial Asia with ~90% confidence. Assessing >2900 hourly OCEC data in 2017–2018 supports the applicability of the PFS indicator to evaluate hourly impacts of PF smoke on receptor urban $PM_{2.5}$ in the Maritime Continent.

© 2019 The Authors. Published by Elsevier Ltd. This is an open access article under the CC BY-NC-ND license (http://creativecommons.org/licenses/by-nc-nd/4.0/).

1. Introduction

The recurrent peat-forest (PF) burning smoke in equatorial Asia (or Maritime Continent), primarily during the southwest monsoon season, can impose significant environmental impacts, accounting for around 3% and 40% of burning-related $PM_{2.5}$ in the world and Southeast (SE) Asia, respectively (GFED, 2017; data for 1997–2016). However, evaluation of associated impacts on public health, ecosystems, and economy at source and receptor locations is impeded by varied burning intensities, unique properties of peat as fuel, evolution of PF smoke during atmospheric transport, interference of local emissions at receptor sites, etc. These complex factors and processes also challenge the applicability of existing findings based on simulated laboratory burning of biomass and field measurements of fire emissions of temperate forests, African savanna, and crop residues in the Indian subcontinent, East Asia, as well as the

☆ This paper has been recommended for acceptance by Eddy Y. Zeng.

* Corresponding author. Department of Civil and Environmental Engineering, National University of Singapore, 1 Engineering Drive 2, 117576, Singapore.
E-mail address: liya.yu@nus.edu.sg (L.E. Yu).

[1] Currently at Department of Earth Sciences, Indian Institute of Science Education and Research (IISER) – Kolkata, Mohanpur 741246, Nadia, West Bengal, India.

[2] Currently at School of Atmospheric Sciences, Sun Yat-Sen University, Guangzhou 510275, People's Republic of China.

https://doi.org/10.1016/j.envpol.2019.02.049
0269-7491/© 2019 The Authors. Published by Elsevier Ltd. This is an open access article under the CC BY-NC-ND license (http://creativecommons.org/licenses/by-nc-nd/4.0/).

Indochina region (northern SE Asia). This is mainly because, differing from the burning of surface vegetation, burning peat in the Maritime Continent often undergoes underground smoldering at a lower temperature for a prolonged duration with occasional flaring (Radojevic, 2003). Such unique burning patterns can invalidate various indicators for burning emissions reported in the literature. For example, indicators involving non-sea-salt potassium (nss-K^+) are typically devised for emission of flaming fires at high temperatures (e.g. ~1000 K) releasing large amounts of nss-K^+. These indicators would not properly represent effects of PF smoke in the Maritime Continent that mainly emits from smoldering at ~500–700 K (Chuang et al., 2013; Wooster et al., 2003) and contains little nss-K^+ (Iinuma et al., 2007; Fujii et al., 2015a).

In addition to unique burning characteristics and fuel types, evolution of the PF smoke during atmospheric transport increases the uncertainty of employing levoglucosan, which is an organic marker emitting from pyrolysis of cellulose and hemicellulose (Simoneit et al., 1999), and can undergo atmospheric oxidation during transport (Hoffmann et al., 2010). Interactions of transported PF smoke with local emissions at receptor sites further complicate the assessment of impacts of PF smoke in the Maritime Continent, especially when receptor environments are insufficiently examined. To build up-to-date understandings, long-term studies of how transported PF smoke affects densely populated large cities in the Maritime Continent are needed, yet lacking. There are only four published work conducting receptor-based studies of PF smoke in Southeast Asia occurring through the past decade (Pavagadhi et al., 2013; Fujii et al., 2015b; Fujii et al., 2016a and b). Although most studies provided snapshots of PF smoke impacts at receptor sites with limited daily sample size or study durations, Fujii et al. (2015b) reported a relatively comprehensive case study of transboundary PF smoke in the Maritime Continent during August 2011–July 2012. Nevertheless, yearly variations in peatland usage, meteorological conditions, and concerns on public exposure and associated health impacts at receptor environments (e.g. large cities) demand longer temporal characterization across multiple years and more rapid detection of transboundary smoke in receptor environment.

To address the abovementioned challenges and needs, this study, as part of the campaign of 7 Southeast Asian Studies (7SEAS), investigates the carbonaceous profile of >260 daily $PM_{2.5}$ samples collected at an urban receptor site (Singapore) and a source site (Jambi, Indonesia) during 2012, 2013 and 2015. The multi-year study duration provides a representative baseline of the urban receptor environment to characterize the influence of transboundary PF smoke on urban $PM_{2.5}$. We examined the carbonaceous profile of four classes of non-smoke-dominant (NSD), smoke-dominant (SD), and episodic samples at an urban receptor site, as well as near-source $PM_{2.5}$ collected at Jambi, Sumatra, Indonesia during 2012–2015. Based on the characteristic profiles of carbon fractions of individual sample groups, we develop a PF smoke (PFS) ratio ((OC2+OC3+POC)/Soot-EC) capable of identifying progressive daily (averaged 24-hr) impacts of PF smoke from source to receptor sites. We further apply the PFS ratio to >2900 hourly data obtained in 2017–2018 to assess its applicability of indicating PF-smoke impacts on the receptor urban environment in the Maritime Continent in a more timely (hourly) fashion.

2. Experimental

2.1. Study location and $PM_{2.5}$ sampling

Singapore is an urbanized and industrialized city-state in SE Asia (Fig. S1(a), Supplementary Material) with a population density of 7737 persons km^{-2} (http://data.worldbank.org/indicator/EN.POP.DNST). It experiences tropical climate with relatively high and uniform temperature (25 °C–32 °C), high relative humidity (~84%) and abundant rainfall (~2330 mm yr^{-1}) (http://www.weather.gov.sg/). There are two monsoon seasons in Singapore; generally, the northeast monsoon ranges from December to March, and the southwest monsoon covers June to September. The urban environment of Singapore is recurrently affected by PF burning smoke in the Maritime Continent, which can be most significant during the southwest monsoon with air masses passing over Sumatra and parts of Borneo.

Filter sampling was conducted on the rooftop of Engineering Block E2 (1°18′N, 103°46′E, 67 m above mean sea level; Fig. S1(b), Supplementary Material) at the National University of Singapore (NUS) during May 2012–June 2013 and June 2015–December 2015. A total of 268 daily (24-h) $PM_{2.5}$ filter samples in 2012–15 were studied in this work. An on-site meteorological station measured temperature, relative humidity (RH), solar insolation, rainfall, wind speed and wind direction every 5 min (https://inetapps.nus.edu.sg/fas/geog/). Daily $PM_{2.5}$ filter samples were collected using three sampling trains coupled with sharp-cut cyclones (URG, USA) operating at a flowrate of 16.7 l min^{-1} for 24 h. One of the sampling trains was equipped with a PTFE filter (Pall, USA) to cater for post-sampling gravimetric measurements and quantification of metals as well as ionic species. Two denuders were assembled upstream of the PTFE filter to minimize positive sampling artifacts by removing acidic and alkaline gases. A nylon filter (Nylasorb, Pall, USA) was installed downstream of the PTFE filter to collect re-vaporized nitrates and chlorides to correct negative sampling artifacts. Downstream to the nylon filter was an additional denuder to correct negative sampling artifacts of ammonium volatilized from the PTFE filter. Gravimetric concentrations were obtained by conditioning the PTFE filters in a desiccator overnight before weighing using a microbalance (Toledo, USA) in a controlled-environment chamber (22 °C, 38% RH).

The other two sampling trains were equipped with a quartz filter (QMA, Whatman, UK) and a TFE-coated glass fiber filter (Fiberfilm, Pall, USA) for subsequent analysis of elemental and organic carbon (EC and OC), and organic speciation, respectively. Prior to sampling, quartz filters were baked at 550 °C for 8 h and the TFE-coated glass fiber filters underwent solvent cleaning to minimize background organic contamination.

Overall, the $PM_{2.5}$ filter samples collected at the receptor site in 2012–15 were classified into three groups, including 104 non-smoke-dominant (NSD) samples, 131 smoke-dominant (SD) samples, and 6 episodic smoke samples (17^{th}–22^{nd} June 2013). Sample categories are classified by assessing the concentration trend in biomarkers of peat-forest smoke (e.g. levoglucosan); an upward concentration trend of PF smoke biomarkers indicates that input mechanisms of biomarkers dominate over their outgoing processes (e.g. rainfall, dilution, oxidation) concerning the urban environment of this study. Sample categories are also classified by adopting air-parcel backward trajectories using HYSPLIT (http://ready.arl.noaa.gov/HYSPLIT.php) and hotspot maps of the Maritime Continent (https://www.nrlmry.navy.mil/aerosol_web/7seas/7seas.html). The criteria of sample classification are detailed in a separate work (Lan et al., 2019). Examples showing hotspot maps overlaid with backward trajectory of air mass corresponding to NSD, SD and episodic sample categories are presented in Fig. 1.

To exclude effects of photochemical reactions on carbonaceous concentrations in fine urban aerosols, a total of 21 nocturnal $PM_{2.5}$ samples were collected at the same location from 7 p.m. to 7 a.m. the next day during May 14–June 11, 2014 when the local ambient environment is under more stagnant conditions. Characteristics of PF smoke $PM_{2.5}$ prior to undergoing substantial regional atmospheric transport and evolution were examined by collecting six

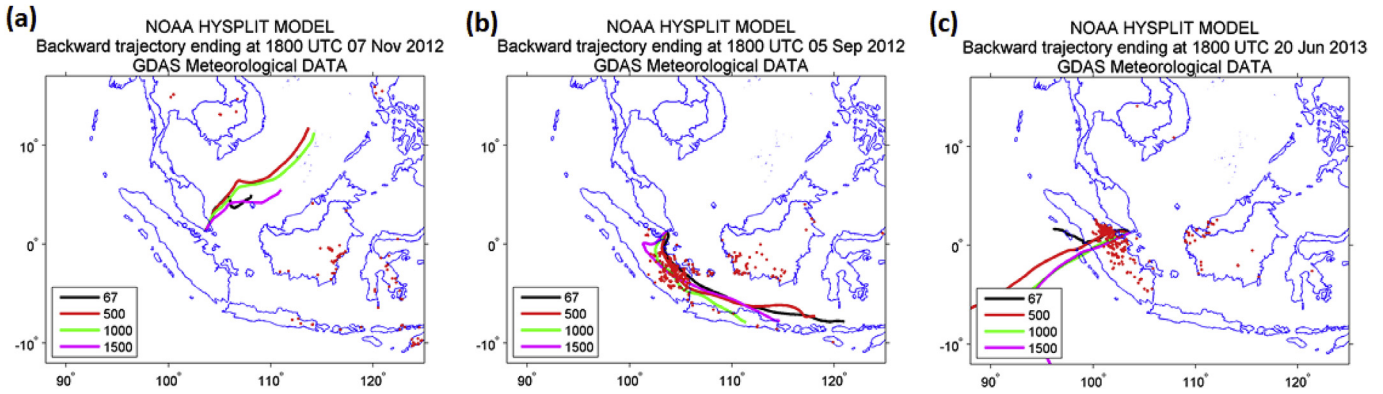

Fig. 1. Examples of overlaid hotspot maps and HYSPLIT air parcel backward trajectories for the receptor urban site during (a) non-smoke dominant (NSD) conditions, (b) smoke-dominant (SD) periods, and (c) episodic samples affected by transboundary PF smoke from Central Sumatra (Riau).

near-source samples at around 2 km downwind from PF burning sites in Jambi, southern Sumatra, Indonesia (1°6′S, 103°8′E'; Fig. S1(a), Supplementary Material) during 27th September–2nd October 2012. A mini-volume sampler (MiniVol™ TAS, Airmetrics, USA) was deployed to collect bulk $PM_{2.5}$ on pre-cleaned quartz filters (QMA, Whatman, UK), and a 5-stage Sioutas Personal Cascade Impactor (SKC, USA) equipped with PTFE-membrane filters (Zefluor, Pall, USA) was deployed to concurrently collect size-segregated PM. The aerosol-loaded filters were stored and frozen in situ in a cryoshipper (CX100, Taylor-Wharton, USA) immediately after sampling, and transported back to our laboratory at NUS for analyses.

2.2. Chemical analyses

To obtain the concentrations of ionic species, PTFE filter (half portion), nylon filter and denuders downstream of the PTFE filter were extracted with 17 ml of ultrapure water (Milli-Q, USA) in an ultrasonication bath for 30 min followed by filtration through a nylon syringe filter with a pore size of 0.45 μm (Environmental Express, USA). The water extracts were analyzed for nine ionic species (Cl^-, NO_3^-, $C_2O_4^{2-}$, SO_4^{2-}, NH_4^+, Na^+, K^+, Ca^{2+} and Mg^{2+}) using a Dionex IC system (Model ICS-3000, Dionex, USA). In this study, only the concentrations of K^+, $C_2O_4^{2-}$ and SO_4^{2-} are employed. For cation analysis, cesium (Cs) was co-injected to monitor and correct inconsistency due to instrument performance. For anion analysis, because of the lack of a suitable co-injection standard, extract samples were re-injected until two quality control criteria were achieved: (i) injections of standard mixture after every 10 analyses of extract samples were consistent with deviation <10%, and (ii) results of every two successive injections of each extract sample were consistent with deviation <10%. The method detection limits (MDL) of quantified $C_2O_4^{2-}$, SO_4^{2-} and K^+ were 2, 28 and 31 ng m^{-3}, respectively.

To quantify carbonaceous materials in $PM_{2.5}$, a 1.5 cm^2 punch of each quartz filter hosting 24-hr integrated fine aerosols was subjected to OC-EC analysis using a thermal/optical analyzer (Sunset Laboratory, USA) employing the IMPROVE_A thermal protocol (Chow et al., 2007) based on reflectance method with correction of carbon pyrolysis. The total carbon (TC) sums OC and EC together. Using blank measurements (Lin et al., 2009), 3σ detection limits of OC and EC are 0.6 μg m^{-3} and 0.001 μg m^{-3}, respectively, showing negligible EC contamination in blanks. However, based on the instrument sensitivity (0.2 μgC cm^{-2}), a corresponding detection limit of 0.13 μg m^{-3} is adopted for both OC and EC in this study. Although quartz filters are known to incur a net positive sampling artifact, overestimating OC concentrations, our regression evaluation and statistical tests (Section S1, Supplementary Material) show that the sampling artifacts are less than significant on both NSD and SD $PM_{2.5}$ samples.

A standard solution of sucrose was used to check instrument performance for analysis of every 10 samples with <10% deviation being the criterion for acceptance. The IMPROVE_A program produces four OC fractions (i.e. OC1–OC4) with step-wise heating up to 580 °C using He as the carrier gas. A continual increase in the temperature up to 840 °C under 98% He/2% O_2 yields the pyrolyzed organic carbon (POC) fraction, which is monitored by a red laser at 632 nm, and three EC fractions (i.e. EC1–EC3). The temperature ramping profiles were retrieved and monitored for consistency. The difference between the amount of EC1 and POC (i.e. excluding POC from EC1) is designated as char-EC, and the sum of EC2 and EC3 (i.e. EC2+EC3) is addressed as soot-EC (Han et al., 2007, 2010). The total amount of OC is defined as the sum of the four OC fractions and POC (i.e. OC1+OC2+OC3+OC4+POC), and the concentration of EC covers all three EC fractions excluding the amount of POC (i.e. EC1+EC2+EC3-POC).

Organic compounds in $PM_{2.5}$ were speciated by extracting TFE-coated glass fiber filters using three types of organic solvents following established methods reported elsewhere (Yang and Yu, 2008; Yang et al., 2013). Briefly, filters were spiked with two internal standards, pre-deuterated tetracosane ($C_{24}D_{50}$) and suberic acid ($C_8H_{14}O_4$), followed by ultrasonic-assisted extraction using tetrahydrofuran, dichloromethane and hexane for 10 min each. Extracts were subsequently filtered through 0.2 μm PTFE syringe filters (Cronus, UK) before a 2-stage concentration step was carried out using a Zymark evaporator (TurboVap II, Zymark Co., USA) and a micro-concentrator (Pierce Inc., USA) to obtain a final extract volume of <300 μl. An aliquot of 50 μl of each solvent extract was drawn and derivatized using 20 μl of N,O-bis(trimethylsilyl)-trifluoroacetamide (BSTFA, Sigma-Aldrich, USA) at room temperature prior to analysis via a GC system (Model 436, Brüker, USA) coupled with a triple-quadrupole mass spectrometer (SCION TQ, Brüker, USA). Injected compounds were separated through a 30 m HP-5 MS column (5% phenyl polysiloxane capillary column, 0.25 mm × 0.25 μm, Agilent) following a temperature profile, which stayed at an initial temperature of 60 °C for 3 min before being increased to 280 °C at a rate of 8 °C min^{-1} and held at 280 °C for 30 min. Helium (99.999%) set at 1.0 ml min^{-1} was used as the carrier gas, and high-purity nitrogen was supplied as a collision gas with a flow rate of 1.5 ml min^{-1}. The mass spectrometer was operated in electron impact (EI) mode at 70 eV with a source temperature of 200 °C. The transfer line temperature was

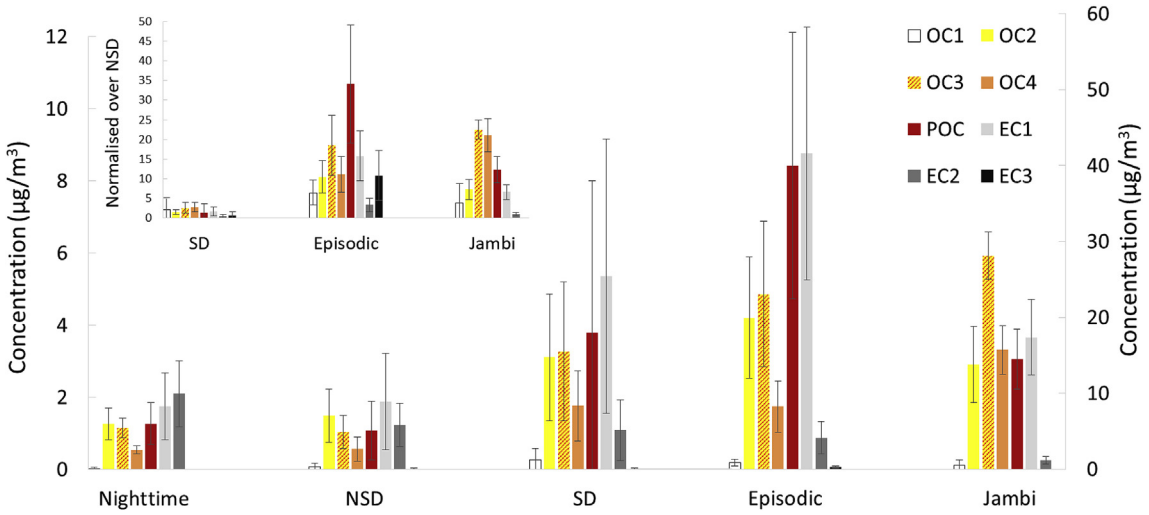

Fig. 2. Carbonaceous profiles (mean±1σ) for individual categories of non-smoke dominant (NSD) nighttime, 24-h bulk NSD, smoke-dominant (SD), episodic and near-source $PM_{2.5}$ (2012–2015). The values of Episodic and Jambi samples follow the secondary y-axis. The inset shows enhancements of each carbonaceous fraction over NSD samples (as baseline).

maintained at 250 °C. The MDL for levoglucosan is 15 ng m^{-3}. Following the same sample preparation procedure, organics in filter samples collected at the receptor site in 2015 and at the near-source site in 2012 were speciated via a GC-MS system (Agilent GC7890-MS5795C) using the same temperature program as for the GC-QqQ system.

3. Results and discussion

3.1. Overall OCEC trend of $PM_{2.5}$ at receptor site

Unlike the rainy season during northeast monsoon (Fig. 1(a)), most transboundary PF smoke in the equatorial Asia affects the receptor site (Singapore) during August and September (Fig. 1(b) as an example), as described in the overview of the dynamics of PF smoke transport in the Maritime Continent (Reid et al., 2012). Because of varied direction of air mass at different altitudes and deep convection mixing in the Maritime Continent, the dominant origins of peat-forest smoke affecting our study site can be best identified in the published literature as central Sumatra, southern Sumatra and/or Borneo regions. In contrast to SD and near-source samples, the episodic samples in 2013 were mainly affected by transboundary smoke from Central Sumatra, Riau, Indonesia. Relative to NSD samples, the transboundary episodic smoke in 2013 increases the mean $PM_{2.5}$ concentration in the urban environment by around eight times (Table 1). The mean concentration of episodic $PM_{2.5}$ at the receptor site in 2013 is even higher than that near PF burning sites in Jambi (in 2012) by ~70% (Table 1), demonstrating the acute severity of this smoke episode. Although the near-source sampling site was directly affected by the smoke envelope of moderate intensity as the light brown envelope shown in Fig. S3(a), the fire radiative power in Sumatra corresponding to our sampling dates in 2012 (176–223 GW) is lower than that in Riau in June 2013 by more than 20% (Gaveau et al., 2014). The uniquely strong burning intensity in Riau was so severe that the thickest smoke blanketed the southern tip of Malaya Peninsula, including the receptor site of this study (Fig. S3(b)) as if Singapore was nearby the burning sites, and thus the smoky episode in the urban environment.

The profile of carbon fractions stands out as one of the most significant characteristics among the four sample categories (Fig. 2). On average, the transboundary PF smoke increased total carbon (TC) of $PM_{2.5}$ collected in 2012–2015 by factors of ~2–15 with mean concentrations of ~6, 15, and 98 μg m^{-3} for NSD, SD and episodic samples, respectively (Table 1). Under strong influence of transboundary PF smoke, OC is responsible for on average 80% and 94% of TC in the SD and episodic samples, respectively (Table 2). This is consistent with large amounts of OC close to the PF burning site we measured in Jambi (southern Sumatra), ranging from 52 to 90 μg m^{-3} and accounting for an average of 95% of TC (Tables 1 and 2), or 49–80% (63 ± 11%) of $PM_{2.5}$ concentration. The abundant OC emitting from PF burning is also supported by Fujii et al. (2014) who measured $PM_{2.5}$ close to burning sites in central Sumatra (Riau) and reported a mean OC fraction of 71 ± 5%.

Transboundary PF smoke introduced much more OC than EC to receptor urban atmosphere. Compared to the NSD samples (as the baseline), mean OC levels for SD and episodic samples are higher by factors of around 3 and 21, respectively. In contrast, the mean EC concentration only accounts for ~4% of SD $PM_{2.5}$, much lower than its fraction (8%) in NSD samples although SD $PM_{2.5}$ hosted more EC (2.7 μg m^{-3}) than NSD samples (2.1 μg m^{-3}) (Table 1). The feature of abundant OC with little EC can be mainly attributed to the low-temperature smoldering of Indonesian PF fires (Fujii et al., 2015a), generating much larger proportions of OC than EC. Lab-scale smoldering of Indonesian peat also reported significantly higher emission factors of OC (6020–8000 mg kg^{-1}) compared to EC (40–570 mg kg^{-1}) (Christian et al., 2003; Iinuma et al., 2007). Thus, such disproportionate and substantial increase in OC compared to EC concentration marks one of the characteristic impacts of transboundary PF smoke on receptor urban aerosols.

3.2. Carbonaceous profile of NSD $PM_{2.5}$ at receptor site

Employing NSD samples as the reference shows progressive impacts of PF smoke from source to receptor site in the Maritime Continent. All the values in brackets represent fractional contribution to the total carbon (TC). With absent or little influence of transboundary PF smoke, the NSD samples were most abundant in EC1 (28%) and OC2 (23%), followed by EC2 (21%) and OC3 (17%) (Table 2). Both EC1 and OC2 together are responsible for > 50% of TC in urban $PM_{2.5}$, indicating dominance of emissions from on-road vehicles, shipping, industrial activities, etc. based on reported profiles (Cao et al., 2006; Jeong et al., 2011; Lim et al., 2012). Published studies also showed that primary emissions and formation of

Table 1
Concentrations (μg m^{-3}) of $PM_{2.5}$, carbonaceous fractions and chemical species for individual sample classes measured during 2012–2015.

Component	Non-smoke dominant nighttime (n = 21)	Non-smoke dominant (n = 104)	Smoke-dominant (n = 131)	Episodic smoke (n = 6)	Jambi near-source (n = 6)
$PM_{2.5}$	NA	25.2 ± 9.3 (11.5–60.4)	60.6 ± 40.8 (22.4–194.6)[1]	199.0 ± 88.3 (87.8–317.0)[2,3]	117.6 ± 26.1 (76.4–153.1)[4,5]
OC1	0.03 ± 0.02 (0.01–0.09)	0.08 ± 0.09 (0–0.50)	0.26 ± 0.31 (0–2.28)[1]	0.89 ± 0.43 (0.51–1.64)[2,3]	0.53 ± 0.67 (0–1.68)
OC2	1.27 ± 0.44 (0.74–2.36)	1.49 ± 0.74 (0.36–3.85)	3.11 ± 1.75 (0.53–11.53)[1]	20.0 ± 8.0 (11.6–33.9)[2,3]	13.8 ± 5.0 (7.0–20.4)[4,5]
OC3	1.16 ± 0.27 (0.78–1.73)	1.03 ± 0.46 (0.43–2.71)	3.27 ± 1.93 (0.93–10.53)[1]	23.1 ± 9.6 (12.5–41.0)[2,3]	28.1 ± 3.1 (23.1–31.9)[4,5]
OC4	0.54 ± 0.11 (0.35–0.85)	0.57 ± 0.34 (0.22–2.43)	1.76 ± 0.98 (0.41–5.01)[1]	8.3 ± 3.4 (5.1–14.6)[2,3]	15.7 ± 3.2 (11.7–20.5)[4,5,6]
EC1	1.75 ± 0.92 (0.75–4.70)	1.89 ± 1.34 (0.39–7.38)	5.35 ± 3.80 (1.05–22.2)[1]	41.6 ± 16.7 (24.3–72.9)[2,3]	17.4 ± 5.0 (10.6–24.6)[4,5,6]
EC2	2.10 ± 0.91 (1.18–4.39)	1.24 ± 0.61 (0.12–3.25)	1.09 ± 0.84 (0.16–4.03)	4.1 ± 2.1 (1.6–7.7)[2,3]	1.17 ± 0.53 (0.60–1.90)[6]
EC3	BD	0.02 ± 0.03 (BD–0.12)	0.02 ± 0.02 (BD–0.09)	0.29 ± 0.17 (0.12–0.60)[2,3]	BD
POC	1.27 ± 0.58 (0.67–2.84)	1.07 ± 0.82 (BD–4.29)	3.79 ± 4.22 (BD–22.2)[1]	40.0 ± 17.6 (21.3–72.9)[2,3]	14.5 ± 3.9 (10.0–20.8)[4,5,6]
OC	4.27 ± 1.33 (2.57–7.52)	4.25 ± 1.91 (1.47–10.0)	12.2 ± 8.3 (2.9–49.7)[1]	92.2 ± 38.7 (51.0–164.0)[2,3]	72.6 ± 14.3 (51.8–90.4)[4,5]
EC	2.58 ± 1.28 (1.17–6.19)	2.07 ± 1.14 (0.71–6.09)	2.67 ± 1.24 (0.85–7.86)[1]	6.0 ± 1.4 (4.7–8.3)[2,3]	4.1 ± 1.6 (1.4–6.0)[4,6]
TC	6.8 ± 2.5 (4.4–13.7)	6.4 ± 2.7 (2.3–14.4)	14.9 ± 8.8 (3.9–53.7)[1]	98.2 ± 40.0 (55.7–172.3)[2,3]	76.7 ± 15.8 (53.1–96.5)[4,5]
Char-EC	0.48 ± 0.46 (BD–1.86)	0.82 ± 0.97 (BD–3.91)	1.56 ± 1.49 (BD–7.64)[1]	1.59 ± 1.04 (BD–2.99)	2.88 ± 1.42 (0.59–4.31)[4]
Soot-EC	2.10 ± 0.91 (1.17–4.39)	1.26 ± 0.61 (0.12–3.26)	1.11 ± 0.85 (0.16–4.08)	4.4 ± 2.3 (1.7–8.3)[2,3]	1.17 ± 0.53 (0.60–1.90)[6]
nss-K^{+}[7]	NA	0.32 ± 0.20 (0.06–1.16)	0.68 ± 0.46 (0.04–3.03)[1]	1.03 ± 0.56 (0.43–2.03)[2]	0.73 ± 0.32 (0.37–1.26) [4]
nss-SO_4^{2-}[8]	NA	4.92 ± 2.90 (1.08–15.7)	8.02 ± 3.79 (2.56–20.8)[1]	5.7 ± 2.9 (2.8–10.1)	10.5 ± 2.2 (8.7–14.7)[4,5,6]
Levoglucosan	NA	0.05 ± 0.02 (0.02–0.13)	0.34 ± 0.32 (0.02–1.61)[1]	6.6 ± 3.1 (3.0–11.1)[2,3]	0.84 ± 0.70 (0.21–2.10)[4,6]
Malic acid	NA	0.03 ± 0.03 (0–0.15)	0.21 ± 0.23 (0.01–1.57)[1]	0.23 ± 0.18 (0.03–0.46)[2]	NA
Oxalate	NA	0.34 ± 0.16 (0.07–0.83)	0.78 ± 0.73 (0.19–4.69)[1]	0.57 ± 0.36 (0.18–1.12)	1.5 ± 1.2 (0.56–3.6)

NA: not analyzed; [1]Significantly different from the values for non-smoke dominant (NSD) $PM_{2.5}$ (*t*-test, $p < 0.05$); [2]Significantly different from the values for NSD $PM_{2.5}$ ($p < 0.05$); [3]Significantly different from the values for SD $PM_{2.5}$ ($p < 0.05$); [4]Significantly different from the values for NSD $PM_{2.5}$ ($p < 0.05$). [5]Significantly different from the values for SD $PM_{2.5}$ ($p < 0.05$). [6]Significantly different from the values for episodic $PM_{2.5}$ ($p < 0.05$). [7]non-sea-salt potassium. [8]non-sea-salt sulfate.

Table 2
Order of abundance among individual carbonaceous fractions in total carbon (TC) of $PM_{2.5}$ from 2012 to 2015.[a]

Non-smoke dominant nighttime (n = 21)	Non-smoke dominant (n = 104)	Smoke-dominant (n = 131)	Episodic smoke (n = 6)	Jambi near-source (n = 6)
EC2 (30%)	EC1 (28%)[b]	EC1 (34%)[b]	EC1 (43%)[b]	OC3 (37%)
EC1 (25%)[b]	OC2 (23%)	OC3 (22%)	POC (40%)	EC1 (22%)[b]
OC2 (19%)	EC2 (21%)	OC2 (22%)	OC3 (23%)	OC4 (21%)
OC3 (18%)	OC3 (17%)	POC (22%)	OC2 (20%)	POC (19%)
POC (18%)	POC (17%)	OC4 (12%)	OC4 (8%)	OC2 (18%)
OC4 (8%)	OC4 (9%)	EC2 (8%)	EC2 (4%)	EC2 (2%)
OC1 (0.4%)	OC1 (1%)	OC1 (2%)	OC1 (1%)	OC1 (1%)
EC3 (0%)	EC3 (0.3%)	EC3 (0.1%)	EC3 (0.3%)	EC3 (0%)
Char-EC (6%)	Char-EC (11%)	Char-EC (13%)	Char-EC (2%)	Char-EC (4%)
Soot-EC (30%)	Soot-EC (21%)	Soot-EC (8%)	Soot-EC (4%)	Soot-EC (2%)
OC (63%)	OC (68%)	OC (80%)	OC (94%)	OC (95%)
EC (37%)	EC (32%)	EC (20%)	EC (6%)	EC (5%)

[a] Values may not add up to 100% due to rounding.
[b] EC1 fraction comprises POC fraction.

secondary organic aerosols (SOA) could contribute to abundant OC2 (Gu et al., 2010; Lim et al., 2012; Diab et al., 2015).

Unlike the 24-h bulk NSD $PM_{2.5}$, the carbonaceous profile of the nocturnal NSD samples in this work is led by EC2 (30%), EC1 (25%) and OC2 (19%) (Table 2). With little or negligible influence of transboundary PF smoke, large amounts of EC could be associated with fossil fuel combustion in the form of diesel combustion (Cao et al., 2006; Andreae and Gelencsér, 2006). The OC2 fraction in the nocturnal NSD samples with a mean concentration of 1.3 μg m^{-3} is 15% lower than that in the 24-h bulk NSD $PM_{2.5}$ (Table 1), possibly due to absent photochemical oxidation and reduced on-road traffic during night-time. However, it is worthwhile to note that carbonaceous concentrations in $PM_{2.5}$ can increase during the night. For example, isoprene can undergo dark ozonolysis forming secondary organic aerosols (Clark et al., 2016), contributing to OC in nocturnal $PM_{2.5}$.

3.3. Carbonaceous profile of SD $PM_{2.5}$ at receptor site

With NSD $PM_{2.5}$ as the baseline, transboundary PF smoke enriched OC3 and OC4 the most, by factors of >3 although EC1, OC3 and OC2 are the three leading carbonaceous fractions in SD samples. The significant increase in these two fractions echoes the profile of near-source samples collected at Jambi, Indonesia, exhibiting OC3 as the most abundant fraction (37%) followed by EC1 and OC4 (Table 2). In fact, OC4 is the second largest fraction in the near-source samples because >85% of EC1 is contributed by the large POC fraction (Table 2). Because organics are more susceptible to oxidation loss during atmospheric transport compared to EC, it is not surprising that mixing transboundary PF smoke with existing airborne components in the urban environment rendered EC1 (34%) including POC (22%), OC3 (22%) and OC2 (22%) as the three most abundant fractions in SD samples (Table 2). It is worthwhile to note that the mean OC2 concentration in the SD $PM_{2.5}$ (3.1 μg m^{-3}) doubles that in the NSD samples (Table 1), suggesting substantial SOA formation through atmospheric evolution of the PF smoke, and hence increasing the concentration of OC2.

The SD samples exhibit an average char-EC concentration higher than NSD samples by almost 90%, and carry statistically more char-EC (1.6 μg m^{-3}) than soot-EC ($p < 0.01$), unlike the NSD samples (Table 1). This demonstrates that the transboundary smoke introduced large amounts of smoldering emissions because soot-EC is typically generated from high temperature flaming fires of biomass (such as some forest fires) (Han et al., 2012; Han et al., 2016). This profile of high char-EC relative to soot-EC of SD $PM_{2.5}$ is also consistent with the trend for near-source samples collected at

Jambi, Indonesia, hosting a mean char-EC concentration more than doubled soot-EC (Table 1).

3.4. Carbonaceous profile of episodic $PM_{2.5}$ at receptor site

Affected by the strong smoke originating from the central Sumatra (Riau) Indonesia, individual carbonaceous fractions in the episodic samples are substantially higher than other sample groups at the receptor, with a mean TC concentration higher by factors of 15 and 6.5 over NSD and SD samples, respectively. In fact, the mean TC of episodic $PM_{2.5}$ at the receptor is higher than that of the near-source samples at Jambi by ~30% (Table 1), demonstrating substantial differences in burning intensities, locations and transport of the PF smoke from Riau versus other PF burning sites in the Maritime Continent. The upsurge in TC of the episodic $PM_{2.5}$ at the receptor site mainly resulted from the abrupt increase in POC, which is responsible for more than 90% of EC1 (Table 2). This also renders EC1 as the most abundant fraction in episodic $PM_{2.5}$, agreeing with laboratory burning of vegetative species including ponderosa pine wood, ponderosa pine needles, white pine needles, sagebrush, excelsior, Dambo grass, Montana grass and tundra core (Chen et al., 2007).

Large POC fraction is the most distinctive feature of the episodic $PM_{2.5}$, suggesting prominent presence of water-soluble organic compounds (WSOC) in general, or humic-like substances (HULIS) in particular. The POC fraction shows a mean concentration of 40.0 $\mu g\ m^{-3}$, 37 times and 10 times of that in NSD and SD $PM_{2.5}$, respectively (Table 1). The high POC fraction is supported by Fujii et al. (2016a) observing larger amounts of POC in total suspended particulates (TSP) collected at a receptor site (Bangi, Malaysia) when the PF smoke was mainly transported from Riau in 2014. Linking WSOC with POC fraction is inferred from an earlier study, reporting that charring of WSOC contributes to 13–66% of POC during thermal analysis (Yu et al., 2002). Associating the POC fraction with HULIS is mainly based on a laboratory study of standard compounds with humic-like functional groups which thermally evolved at >580 °C (Miyazaki et al., 2007), consistent with the major hosting fractions of OC3, OC4 and POC fractions when we examined using the IMPROVE_A temperature program. Although these HULIS can be emitted as primary components in PF smoke (Hoffer et al., 2006), their presence in the high POC fraction of our episodic $PM_{2.5}$ at the receptor could significantly result from SOA formation during atmospheric transport because little POC was observed in $PM_{2.5}$ collected ~1.5 m from burning sites in Riau during May and June in 2012 (Fujii et al., 2014). Contribution of SOA to the high POC concentration can also be supported by the substantially enhanced concentration of a secondary organic species (malic acid) in the episodic samples, showing a mean concentration up to almost 8 times of that in the NSD $PM_{2.5}$ (Table 1). This agrees with our earlier measurements that substantial increase in malic acid accompanies the presence of transboundary PF smoke in the same receptor urban environment (Yang et al., 2013).

3.5. Carbonaceous profile of $PM_{2.5}$ near PF burning sites

The carbonaceous $PM_{2.5}$ collected near PF burning sites (near-source samples) at Jambi showed dominant OC3 (37%), followed by EC1 (22%), OC4 (21%), POC (19%) and OC2 (18%) (Table 2). This differs markedly from the profile of PF smoke reported by Fujii et al. (2014) who collected samples ~1.5 m away from hotspots at Riau, Indonesia and showed predominant OC1 (32%) and OC2 (48%) fractions. The dominance in the two OC1 and OC2 fractions at the burning site in situ is similar to carbonaceous profiles of fresh smoke emitted from lab-scale burning of pine wood, mesquite, Tamarisk, Huisache, grass, maize residue, etc. (Chow et al., 2004; Cao et al., 2005). Since the OC1 and OC2 fractions mostly comprise compounds of higher volatility, they can be rapidly depleted downwind during atmospheric transport of the smoke plume. Even at a distance of several hundred meters away from grass and pine forest fires, Chuang et al. (2013) reported that these highly volatile fractions were substantially lowered in concentrations, rendering OC3 and OC4 as the most abundant fraction. Thus, it is not surprising that after atmospheric transport of around 2 km from the burning sites at Jambi, OC3 tops among carbonaceous fractions in our $PM_{2.5}$ samples (Table 2), indicating a young smoke evolving from fresh PF burning emissions.

3.6. Comparison of carbonaceous profiles among sample classes

Across all sample classes, the most outstanding feature is the systematic increase in OC3 and OC4 concentrations with stronger influence of PF smoke (Fig. 2). Concentrations of OC3 and OC4 increase progressively from NSD to episodic samples at the receptor site, and peak in the near-source $PM_{2.5}$ collected at Jambi (Table 1), concurrent with the enhanced dominance of PF smoke in the atmosphere. Relative to the NSD $PM_{2.5}$, the mean concentrations of OC3 in the SD, episodic, and near-source samples are enriched by factors of 3, 22, and 27, respectively (Inset, Fig. 2). Similarly, the mean OC4 concentrations are raised by respective factors of 3, 14, and 27 (Inset, Fig. 2). It is expected that PF smoke can greatly enrich the OC3, OC4 and POC fractions since thermal degradation products of cellulose and lignin, such as phenols, methoxyphenols (guaiacol, methylguaiacol) etc. mainly evolve in the OC3 fraction at 280°C–480 °C (Grabowsky et al., 2011). Our laboratory studies adopting IMPROVE_A thermal/optical analyses also showed that compounds containing humic-like functional groups and multi-carboxylic acids evolve primarily in fractions of OC3, OC4 and POC. Thus, with NSD urban aerosols as the baseline, an increase in both OC3 and OC4 fractions by a factor of >3 can reflect dominant effects of PF smoke on the receptor urban environment, and a factor of >10 episodic influence. In view of changing atmospheric environments, such assessments are valid when baseline profiles are established with sufficient amounts of sample size.

Other than concurrent enhancement in OC3 and OC4 fractions, there are two additional similarities between SD and near-source $PM_{2.5}$, indicating significant influence of transboundary PF fire emissions from southern Sumatra on urban aerosols at the receptor site. Firstly, both sample classes show OC3 and EC1 as the two most dominant carbonaceous fractions (Table 2). Since EC1 includes POC, both OC3 and POC are consistently most abundant for both sample classes (Table 2). The higher char-EC concentration than soot-EC underscores the second additional resemblance between the SD and near-source samples. The mean char-EC concentration is more than twice the soot-EC near the burning site at Jambi (Table 1), indicating smoldering as the more dominant form of PF burning over flaming. This is not surprising, considering smoldering biomass emits disproportionately higher char-EC compared to soot-EC (Arora and Jain, 2015). Thus, a combination of a larger concentration of char-EC over soot-EC, and OC3 comparable to or over POC in $PM_{2.5}$ at the receptor site may suggest southern Sumatra as one of the major origins of transboundary PF smoke in the urban receptor environment. On the other hand, a reversed fraction profiles showing higher soot-EC than char-EC, and POC than OC3 at the urban receptor may imply other burning sites (e.g. Riau) as the main source locations of PF smoke. This is demonstrated by the episodic $PM_{2.5}$ at the receptor site, which have soot-EC concentration more than double of char-EC (Table 1). This also indicates that the smoke originating from Riau was predominantly emitted from flaming combustion, featuring more abundant POC than OC3, in contrast to the near-source samples at Jambi (Table 2).

Nevertheless, continual monitoring of PF burning, smoke characteristics, land use changes, etc. in the future is needed to further substantiate the observations.

3.7. Proposed indicator of transboundary peat-forest smoke

To characterize effects of transboundary PF smoke on urban receptor environment in the Maritime Continent, Table 3 summarizes the applicability of seven indicator ratios available in published literature, namely OC/EC, char-EC/soot-EC, nss-SO_4^{2-}/EC, nss-K^+/EC, nss-K^+/Levoglucosan, OC/Levoglucosan and POC/OC4. Most ratios reflect urban features in this study, consistent with published values. However, these existing indicators generally yield random orders among sample groups under varied impacts of PF smoke in this study (Table 4). This is mainly because the PF smoke in the Maritime Continent differs significantly from reported burning emissions of other types of biomass. The unique PF smoke properties are further complicated by subsequent evolution during atmospheric transport and interactions with emissions at receptor sites. Additional discussion on the application of these indicators to this study is provided in Section S2 of the Supplementary Material.

Taking advantage of the distinct carbonaceous profiles of the four sample groups in this study, we propose a ratio of summed concentrations of OC2, OC3 and POC to soot-EC concentration as a PF smoke (PFS) indicator to differentiate the characteristic impacts of PF smoke (PFS) on the individual sample classes. The three components in the numerator exhibit abundant enrichment by PF smoke relative to the NSD samples. The OC4 fraction is not included in the numerator for its concentration is much lower than other OC fractions. The denominator, soot-EC, is selected because its airborne concentrations depend mainly on primary emissions and deposition removal prior to reaching receptor sites (Han et al. 2009; 2010) with little influence of secondary atmospheric processes. Lesser soot-EC fraction (<10%) in the TC of PF smoke significantly differs from that (>20%) of exhausts associated to anthropogenic activities operating at high temperature combustion (e.g. on-road traffic and industrial processes) (Table 2). Hence, incorporating soot-EC numerically widens the differences among resultant PFS ratios, and thus offers better distinction among individual sample groups. The mean PFS ratio of individual sample classes progressively increases with stronger PF smoke influences with statistical significance ($p < 0.01$), rendering the largest value of 54.7 representing near-source $PM_{2.5}$ followed by episodic $PM_{2.5}$ (20.1 ± 4.1), SD (13.4 ± 11.6), NSD (3.6 ± 3.6), and nocturnal NSD (1.9 ± 0.4) at the urban receptor site (Table 4).

The temporal trend of the PFS ratio at the receptor site satisfactorily follows that of levoglucosan (Fig. 3) with a Pearson correlation of 0.78, 0.92, and 0.78 in respective years 2012, 2013 and 2015. This indicates the feasibility of using the indicator to differentiate effects of PF smoke on fine aerosols at urban receptors in equatorial Asia. Although levoglucosan can undergo oxidation during atmospheric transport, its surged concentration at receptor sites qualitatively warrant the dominant presence of smoke emitting from biomass pyrolysis. Based on the 268 daily $PM_{2.5}$ samples in this study, when a threshold PFS ratio of $\geq$6 is used to determine transboundary PF smoke in the Maritime Continent as the dominant factor affecting receptor urban $PM_{2.5}$, an accuracy of ~80% is achieved; or as a worse-case scenario, 20% of urban $PM_{2.5}$ samples will have transboundary PF smoke overlooked as the major influence, because 28 out of 131 SD samples have a PFS ratio <6. As an alternative, employing a criterion of PFS indicator of $\geq$5 can identify the dominant influence of transboundary PF smoke on urban $PM_{2.5}$ with an accuracy of ~90%. To reduce unnecessary false alarms biased by little soot-EC as the denominator of the PFS indicator, we suggest application of the PFS indicator to data sets having a soot-EC concentration >0.2 $\mu g\, m^{-3}$. This value is around the mean of soot-EC concentrations in SD $PM_{2.5}$ minus its 1σ (1.11 ± 0.85, Table 1). It is worth noting that the PFS indicator is more suitable for receptors having little emissions of domestic biomass burning. Caution should also be exercised to evaluate the resultant PFS ratio, in cases of unusual release of large amounts of organic compounds, enlarging the numerator and resulting in large values of PFS ratio. Such unusual cases can be discerned when sufficient knowledge about emissions profiles of baseline cases and meteorological conditions of receptor sites is built.

To identify transboundary PF smoke in the receptor urban environment more rapidly, we examined a total of 2973 hourly carbonaceous profile of $PM_{2.5}$ obtained from a field OCEC thermal/optical analyzer (Model 4G Field Analyzer, Sunset Laboratory Inc., U.S.A.) during November 2017 to August 2018. Since field OCEC thermal/optical analyzers tend to underestimate amounts of carbon (Malaguti et al., 2015), it is necessary to regularly benchmark the measurement values against bulk filter-based offline OCEC data. To ensure that the indication of hourly PFS ratios is consistent with the evaluation established based on daily (24-h) bulk filter data, on each hour, we assess a mean of 24 consecutive individual hourly PFS values up to the hour of interest. As an example, Fig. S4 shows the 24-hr averaged hourly PFS values and hourly PFS values. When transboundary PF smoke is not the dominant factor affecting the urban environment, aggregating 24 hourly data yields a mean hourly PFS ratio of 2.3 ± 0.8 (1.0–4.6), consistent with that of the 24-hr bulk NSD $PM_{2.5}$ samples in 2012–2015 (3.6 ± 3.6, Table 4). In contrast, the hourly 24-hr mean PFS indicator in August 2018 ranges from 5.1 to 14.3, and in general concurs with the

Table 3
Applicability of indicators available in published literature to identify peat-forest smoke impacts on $PM_{2.5}$ collected at near burning sources and receptor sites in the Maritime Continent during 2012–2015.

Indicator ratios	Urban emission[a]	Peat-forest smoke impact	
		Urban receptor site[b]	Near-source vs. receptor site[c]
OC/EC	✓	✓	×
Char-EC/Soot-EC	✓	×	×
nss-SO_4^{2-}/EC	✓	×	×
nss-K^+/EC	✓	×	×
nss-K^+/Levoglucosan	NA	✓	×
OC/Levoglucosan	NA	✓	×
POC/OC4	NA	×	×

NA: Not applicable.
[a] Tick ("✓"): Mean values of NSD $PM_{2.5}$ in this study are consistent with those for typical urban emissions (e.g., on-road vehicle exhaust, industrial activities, etc.) reported in the literature.
[b] Tick ("✓"): There is systematic trend and statistically significant differences ($p < 0.05$) among NSD, SD and episodic $PM_{2.5}$ collected at the receptor urban site.
[c] Tick ("✓"): There is systematic and statistically significant differences ($p < 0.05$) among all NSD, SD and episodic $PM_{2.5}$ at the receptor, and near-source $PM_{2.5}$.

Table 4
Indicator ratios (mean±1σ) applied to individual sample categories in this study (2012–2015) and reported by previously published studies.

Location	(OC2+OC3+POC)/Soot-EC (PFS indicator)	OC/EC	Char-EC/Soot-EC	nss-SO_4^{2-}/EC	nss-K^+/EC	nss-K^+/Levoglucosan	OC/Levoglucosan	POC/OC4
This study (Singapore)								
NSD[a] nighttime	1.9 ± 0.4 (1.2–2.7)	1.8 ± 0.6 (1.2–3.1)	0.21 ± 0.17 (BD–0.47)					2.3 ± 0.6 (1.5–3.5)
NSD	3.6 ± 3.6 (1.0–31.2)	2.3 ± 1.0 (0.9–5.7)	1.0 ± 1.6 (BD–7.0)	2.6 ± 1.5 (0.6–7.1)	0.17 ± 0.12 (0.01–0.55)	9.0 ± 7.6 (1.0–41.0)	116.1 ± 77.8 (22.4–464.7)	2.1 ± 1.2 (BD–6.4)
SD[b]	13.4 ± 11.6 (2.7–82.4)	4.8 ± 2.5 (1.1–12.6)	4.1 ± 5.6 (BD–34.7)	3.4 ± 1.8 (0.6–9.4)	0.29 ± 0.23 (0.01–1.49)	3.6 ± 5.5 (0.03–55.2)	49.1 ± 46.6 (8.9–492.3)	2.3 ± 1.6 (BD–5.2)
Episodic	20.1 ± 4.1 (15.8–27.1)	14.9 ± 2.9 (10.9–19.8)	0.59 ± 0.64 (BD–1.8)	0.93 ± 0.42 (0.50–1.71)	0.17 ± 0.07 (0.09–0.25)	0.18 ± 0.10 (0.07–0.33)	15.3 ± 5.0 (8.8–20.8)	4.8 ± 0.5 (4.2–5.5)
This study (Jambi, Indonesia)								
Near PF fires	54.7 ± 19.9 (27.8–85.2)	20.4 ± 8.7 (15.0–38.0)	2.8 ± 1.9 (0.8–5.9)	3.1 ± 1.8 (1.9–6.7)	0.22 ± 0.14 (0.06–0.42)	1.6 ± 1.4 (0.3–3.9)	141.3 ± 88.0 (35.7–246.5)	0.9 ± 0.2 (0.8–1.2)
Literature studies								
Near PF fires								
Riau, Indonesia[1,2]		36.4 ± 9.1			0.02[3]	0.005±0.006[3]	10.6 ± 2.0	
Riau, Indonesia[4,5,6]		2.4		0.10	0.04			
Transported PF smoke								
St. John's Island, Singapore[6,7,8]		15.5		8.5	0.70	1.4	29.2	
Southwest Singapore[6,9]		2.8		2.9	0.39			
Kula Lumpur, Malaysia[8,10]		13.5					5.5	
Bangi, Malaysisa[6,11]		2.7 ± 0.9	14.5		0.21			7.4 ± 3.4
Bangi, Malaysia[6,8,12,13]		9.7		1.8	0.26	1.7	63.4	11.9–3.6
Palangkaraya, Indonesia[6,14,15,16]		8.1–14.7		1.8–2.7	0.20–0.21			

[1]Fujii et al. (2014); [2]Samples collected ~1.5 m away from peat fires; [3]Fujii et al. (2015a); [4]See et al. (2007); [5]Samples collected ~100 m away from peat fires; [6]Total K^+ and SO_4^{2-} used for calculation; [7]Engling et al. (2014); [8]TSP instead of $PM_{2.5}$; [9]See et al. (2006); [10]Radzi Bin Abas et al. (2004); [11]Fujii et al. (2016); [12]Values refer to Period I only; OC, EC and levoglucosan values estimated from plots and values of corresponding ratios calculated are thus approximate; K^+ and SO_4^{2-} values calculated as mean of the range provided; [13]Fujii et al. (2016); [14]PM_{10} instead of $PM_{2.5}$; [15]Range for 2011 and 2012 reported here; [16]Hayasaka et al. (2014).

[a] NSD: non-smoke dominant.

[b] SD: smoke dominant.

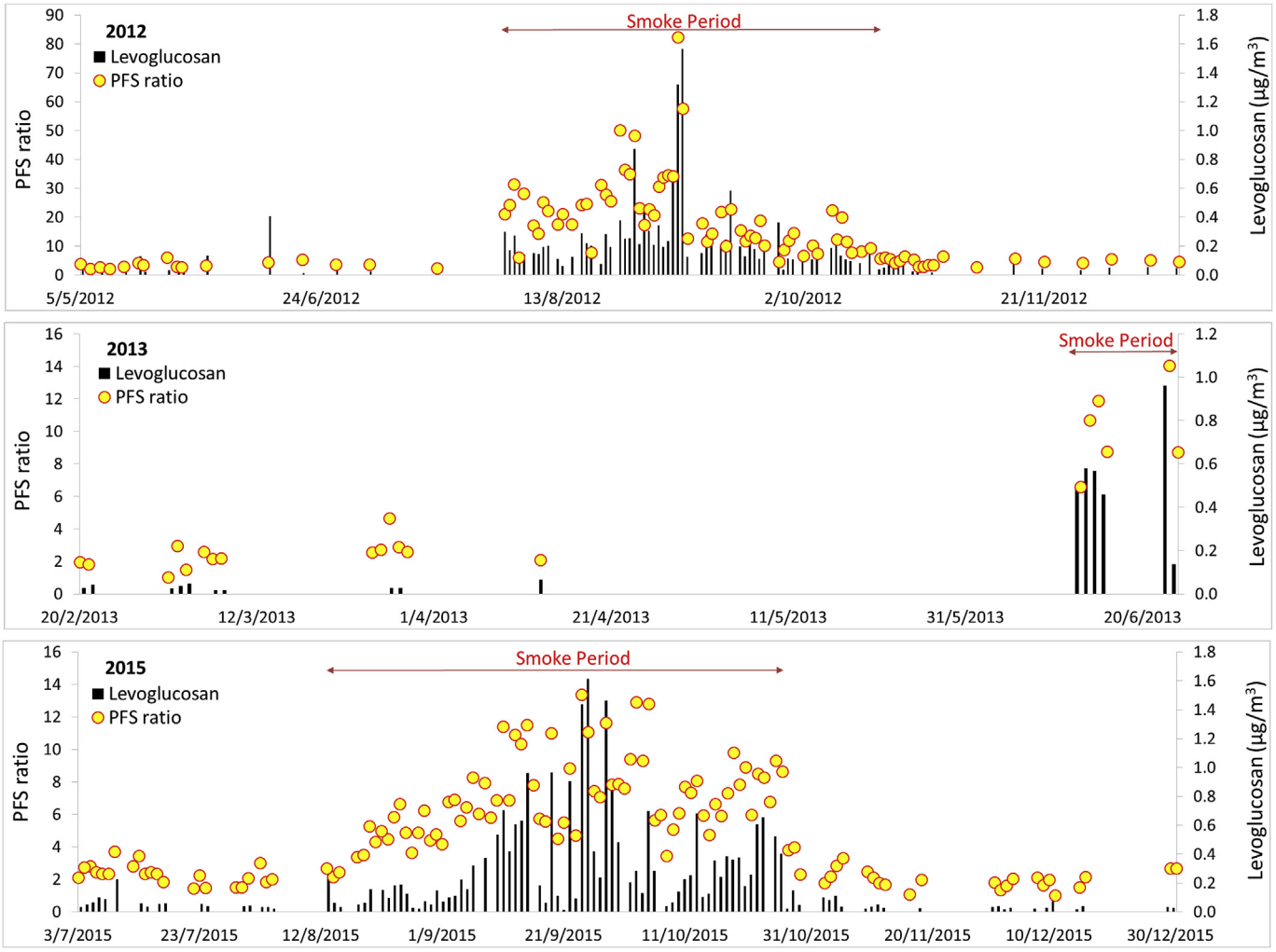

Fig. 3. Temporal trend of the proposed PFS indicator and the concentration of organic tracer (levoglucosan) in $PM_{2.5}$ during 2012–2015. For visual clarity, episodic samples are excluded from the plot of 2013.

corresponding hotspot counts of peat-forest burning in the region (Fig. S5), suggesting that, at any hour, if the mean of consecutive 24 hourly PFS indicator reaches ≥5, PF smoke can exert a dominant influence on urban fine aerosols. This demonstrates potential applicability of adopting the PFS indicator for more timely (hourly) assessment of the influence of transboundary PF smoke on the receptor urban $PM_{2.5}$ in the equatorial Asia.

4. Conclusions

Profiles of carbonaceous aerosol comprising eight fractions of OC and EC and organic markers for biomass burning of 268 daily $PM_{2.5}$ filter samples during 2012–2015 were examined to characterize impacts of peat-forest (PF) smoke from source to receptor sites in the Maritime Continent. We characterized distinctive fractional composition for four sample groups of non-smoke-dominant (NSD), smoke-dominant (SD), and episodic $PM_{2.5}$ at a receptor urban site, as well as for near-source fine particulates at Jambi (Indonesia). Transboundary PF smoke increases average OC concentration in urban $PM_{2.5}$ by up to 20 times with a mean concentration, responsible for 80% and 94% of total carbon (TC) in SD and episodic $PM_{2.5}$, respectively. This is consistent with the abundant OC ($63 \pm 11\%$, 52–90 $\mu g\, m^{-3}$) in $PM_{2.5}$ close to the burning site in Jambi, accounting for 94–97% (95 ± 1%) of TC. The most outstanding feature across all sample classes relative to the receptor baseline is the systematic increase in OC3 and OC4 concentrations with stronger influence of PF smoke; the mean concentration of (OC3+OC4) together increased progressively from NSD samples (1.6 $\mu g\, m^{-3}$) to SD samples (5.0 $\mu g\, m^{-3}$) and episodic $PM_{2.5}$ (31.3 $\mu g\, m^{-3}$) at the receptor site, with the highest concentration (43.8 $\mu g\, m^{-3}$) near the PF burning site. Relative to the NSD $PM_{2.5}$, transboundary PF smoke increased both OC3 and OC4 fractions by factors of >3 and > 14 for SD and episodic cases, respectively. Episodic $PM_{2.5}$ at the receptor is featured with the largest fraction of pyrolyzed organic carbon (POC), responsible for 40% of TC on average, and higher than other urban sample classes by factors of >10 times. The large POC fraction, an indication of the strong tendency of episodic $PM_{2.5}$ undergoing pyrolysis during thermal/optical analyses, also reflects the unique influence of transboundary PF smoke. The carbonaceous profile of SD $PM_{2.5}$ in the receptor environment resembles that of near-source samples in Jambi by having both OC3 and EC1 as the most abundant fractions. In addition, both sample groups show a mean char-EC concentration significantly higher than soot-EC, showing dominant emission of smoldering over flaming.

Considering all the samples (268) measured across 2012–2015, the mean ratio of PF smoke (PFS) indicator satisfactorily identifies influence of PF smoke in the Maritime Continent. The PFS indicator progressively and significantly ($p < 0.01$) increases from 1.9 for nocturnal NSD and 3.6 for NSD 24-hr bulk samples to 13.4 and 20.1

for respective SD and episodic $PM_{2.5}$ at the receptor site, and peaks at 54.7 for near-source fine particulates. A criterion PFS ratio of $\geq$5 is proposed to indicate dominant influence of transboundary PF smoke on urban $PM_{2.5}$ with an accuracy of >90%. A total of 2973 hourly OCEC measured in 2017–2018 support the applicability of this PFS indicator for daily and hourly assessment of impacts of transboundary PF smoke on urban atmosphere in the Maritime Continent.

Acknowledgement

The on-line meteorological data are provided free of charge by Prof. M. Roth at the National University of Singapore (NUS). Dr. Reid's participation was funded by the Naval Research Laboratory Base Research Program. This study (R-706-000-032-133 and R-706-000-043-490) is supported by Provost Office, NUS, Singapore, and the Singapore National Environment Agency (NEA). This work does not represent the view of NEA.

Appendix A. Supplementary data

Supplementary data to this article can be found online at https://doi.org/10.1016/j.envpol.2019.02.049.

References

Andreae, M.O., Gelencsér, A., 2006. Black carbon or brown carbon? The nature of light-absorbing carbonaceous aerosols. Atmos. Chem. Phys. 6, 3131–3148.
Arora, P., Jain, S., 2015. Estimation of organic and elemental carbon emitted from wood burning in traditional and improved cookstoves using controlled cooking test. Environ. Sci. Technol. 49, 3958–3965.
Cao, J.J., et al., 2006. Characterization of roadside fine particulate carbon and its eight fractions in Hong Kong. Aerosol and Air Quality Research 6, 106–122.
Cao, J.J., et al., 2005. Characterization and source apportionment of atmospheric organic and elemental carbon during fall and winter of 2003 in Xi'an, China. Atmos. Chem. Phys. 5, 3127–3137.
Chen, L.W.A., et al., 2007. Emissions from laboratory combustion of wildland fuels: emission factors and source profiles. Environ. Sci. Technol. 41, 4317–4325.
Chow, J.C., et al., 2004. Source profiles for industrial, mobile and area sources in the big bend regional aerosol visibility and observational study. Chemosphere 54, 185–208.
Chow, J.C., et al., 2007. The IMPROVE_A temperature protocol for thermal/optical carbon analysis: maintaining consistency with a long-term database. J. Air Waste Manag. Assoc. 57, 1014–1023.
Christian, T.J., et al., 2003. Comprehensive laboratory measurements of biomass-burning emissions: 1. Emissions from Indonesian, African, and other fuels. J. Geophys. Res. 108, 4719. https://doi.org/10.1029/2003JD003704.
Chuang, M.T., et al., 2013. Characterization of aerosol chemical properties from near-source biomass burning in the northern Indochina during 7-SEAS/Dongsha experiment. Atmos. Environ. 78, 72–81.
Clark, C.H., et al., 2016. Temperature effects on secondary organic aerosol (SOA) from the dark ozonolysis and photo-oxidation of isoprene. Environ. Sci. Technol. 50, 5564–5571. https://doi.org/10.1021/acs.est.5b05524.
Diab, J., et al., 2015. Hyphenation of a EC/OC thermal–optical carbon analyzer to photo-ionization time-of-flight mass spectrometry: an off-line aerosol mass spectrometric approach for characterization of primary and secondary particulate matter. Atmospheric Measurement Techniques 8, 3337–3353.
Engling, G., He, J., Betha, R., Balasubramanian, R., 2014. Assessing the regional impact of Indonesian biomass burning emissions based on organic molecular tracers and chemical mass balance modeling. Atmos. Chem. Phys. 14, 8043–8054.
Fujii, Y., et al., 2014. Characteristics of carbonaceous aerosols emitted from peatland fire in Riau, Sumatra, Indonesia. Atmos. Environ. 87, 164–169.
Fujii, Y., et al., 2015a. Characteristics of carbonaceous aerosols emitted from peatland fire in Riau, Sumatra, Indonesia (2): identification of organic compounds. Atmos. Environ. 110, 1–7.
Fujii, Y., et al., 2016a. A key indicator of transboundary particulate matter pollution derived from Indonesian peatland fires in Malaysia. Aerosol and Air Quality Research 16, 69–78.
Fujii, Y., Mahmud, M., Tohno, S., Okuda, T., Mizohata, A., 2016b. A case study of $PM_{2.5}$ characterization in Bangi, Selangor, Malaysia during the southwest monsoon season. Aerosol and Air Quality Research 16, 2685–2691.
Fujii, Y., et al., 2015b. Annual variations of carbonaceous $PM_{2.5}$ in Malaysia: influence by Indonesian peatland fires. Atmos. Chem. Phys. 15, 13319–13329.
Gaveau, D.L.A., et al., 2014. Major atmospheric emissions from peat fires in Southeast Asia during non-drought years: evidence from the 2013 Sumatran fires. Sci. Rep. https://doi.org/10.1038/srep06112.
GFED, 2017. Global fire emissions database version 4.1 including small fire burned area (GFED4s). Available online at: http://www.globalfiredata.org/. (Accessed 17 July 2017).
Grabowsky, J., et al., 2011. Hyphenation of a carbon analyzer to photo-ionization mass spectrometry to unravel the organic composition of particulate matter on a molecular level. Anal. Bioanal. Chem. 401, 3153–3164.
Gu, J., et al., 2010. Characterization of atmospheric organic carbon and element carbon of $PM_{2.5}$ and PM_{10} at Tianjin, China. Aerosol and Air Quality Research 10, 167–176.
Han, Y., et al., 2007. Evaluation of the thermal/optical reflectance method for discrimination between char- and soot-EC. Chemosphere 69, 569–574.
Han, Y.M., Lee, S.C., Cao, J.J., Ho, K.F., An, Z.S., 2009. Spatial distribution and seasonal variation of char-EC and soot-EC in the atmosphere over China. Atmos. Environ. 43, 6066–6073.
Han, Y.M., Cao, J.J., Lee, S.C., Ho, K.F., An, Z.S., 2010. Different characteristics of char and soot in the atmospheric and their ratio as an indicator for source identification in Xi'an, China. Atmos. Chem. Phys. 10, 595–607.
Han, Y.M., Marlon, J.R., Cao, J.J., Jin, Z.D., An, Z.S., 2012. Holocene linkages between char, soot, biomass burning and climate from Lake Daihai, China. Glob. Biogeochem. Cycles 26. https://doi.org/10.1029/2011GB004197. GB4017.
Han, Y.M., et al., 2016. Climate and fuel controls on North American Paleofires: smoldering to flaming in the late-glacial Holocene transition. Sci. Rep. https://doi.org/10.1038/srep20719.
Hayasaka, H., Noguchi, I., Putra, E.I., Yulianti, N., Vadrevu, K., 2014. Peat-fire-related air pollution in Central Kalimantan, Indonesia. Environ. Pollut. 195, 257–266.
Hoffer, A., et al., 2006. Optical properties of humic-like substances (HULIS) in biomass-burning aerosols. Atmos. Chem. Phys. 6, 3563–3570.
Hoffmann, D., Tilgner, A., Iinuma, Y., Herrmann, H., 2010. Atmospheric stability of levoglucosan: a detailed laboratory and modeling study. Environ. Sci. Technol. 44, 694–699.
Iinuma, Y., et al., 2007. Source characterization of biomass burning particles: the combustion of selected European conifers, African hardwood, savanna grass, and German and Indonesian peat. J. Geophys. Res. 112 https://doi.org/10.1029/2006JD007120. D08209.
Jeong, C.-H., et al., 2011. Receptor model based identification of $PM_{2.5}$ sources in Canadian cities. Atmos. Pollution Res. 2, 158–171.
Lan, Y., et al., 2019. Effects of Transboundary Peat-Forest Smoke on an Urban Environment in Maritime Continent: Long-Term Observations and Insights (in preparation).
Lim, S., et al., 2012. Ionic and carbonaceous compositions of PM_{10}, $PM_{2.5}$ and $PM_{1.0}$ at Gosan ABC Superstation and their ratios as source signature. Atmos. Chem. Phys. 12, 2007–2024.
Lin, P., et al., 2009. Seasonal and diurnal variations of organic carbon in $PM_{2.5}$ in Beijing and the estimation of secondary organic carbon. J. Geophys. Res. 114 https://doi.org/10.1029/2008JD010902. D00G11.
Malaguti, A., et al., 2015. Comparison of online and offline methods for measuring fine secondary inorganic ions and carbonaceous aerosols in the central mediterranean area. Aerosol and Air Quality Research 15, 2641–2653. https://doi.org/10.4209/aaqr.2015.04.0240.
Miyazaki, Y., et al., 2007. Chemical characteristics of water-soluble organic carbon in the Asian outflow. J. Geophys. Res. 112 https://doi.org/10.1029/2007JD009116. D22S30.
Pavagadhi, S., Betha, R., Venkatesan, S., Balasubramanian, R., Hande, M.P., 2013. Physicochemical and toxicological characteristics of urban aerosols during a recent Indonesian biomass burning episode. Environ. Sci. Pollut. Control Ser. 20, 2569–2578.
Radojevic, M., 2003. Chemistry of forest fires and regional haze with emphasis on Southeast Asia. Pure Appl. Geophys. 160, 157–187.
Radzi Bin Abas, M., et al., 2004. Organic composition of aerosol particulate matter during a haze episode in Kuala Lumpur, Malaysia. Atmos. Environ. 38, 4223–4241.
Reid, J.S., et al., 2012. Multi-scale meteorological conceptual analysis of observed active fire hotspot activity and smoke optical depth in the Maritime Continent. Atmos. Chem. Phys. 12, 2117–2147.
See, S.W., Balasubramanian, R., Rianawati, E., Karthikeyan, S., Streets, D.G., 2007. Characterization and source apportionment of particulate matter $\leq$2.5 μm in Sumatra, Indonesia, during a recent peat fire episode. Environ. Sci. Technol. 41, 3488–3494.
See, S.W., Balasubramanian, R., Wang, W., 2006. A study of the physical, chemical, and optical properties of ambient aerosol particles in Southeast Asia during hazy and nonhazy days. J. Geophys. Res. 111, D10S08. https://doi.org/10.1029/2005JD006180.
Simoneit, B.R.T., et al., 1999. Levoglucosan, a tracer for cellulose in biomass burning and atmospheric particles. Atmos. Environ. 33, 173–182.
Wooster, M.J., Zhukov, B., Oertel, D., 2003. Fire radiative energy for quantitative study of biomass burning: derivation from the BIRD experimental satellite and comparison to MODIS fire products. Rem. Sens. Environ. 86, 83–107.
Yang, L., Nguyen, D.M., Jia, S., Reid, J.S., Yu, L.E., 2013. Impacts of biomass burning smoke on the distributions and concentrations of C_2-C_5 dicarboxylic acids and dicarboxylates in a tropical urban environment. Atmos. Environ. 78, 211–218.
Yang, L., Yu, L.E., 2008. Measurements of oxalic acid, oxalates, malonic acid, and malonates in atmospheric particulates. Environ. Sci. Technol. 42, 9268–9275.
Yu, J.Z., Xu, J., Yang, H., 2002. Charring characteristics of atmospheric organic particulate matter in thermal analysis. Environ. Sci. Technol. 36, 754–761.